

A revised model for circumstellar molecular emission

M.A.T. Groenewegen^{1,2}

¹ Astronomical Institute ‘Anton Pannekoek’, Kruislaan 403, NL-1098 SJ Amsterdam, The Netherlands

² Present address: Institut d’Astrophysique de Paris, 98bis Boulevard Arago, F-75014 Paris, France

Received 2 September 1993 / Accepted 8 March 1994

Abstract. A model is presented to calculate the line profiles of thermal emission of molecules in an expanding spherically symmetric circumstellar envelope. Special attention is given to the heating and cooling mechanisms which determine the kinetic temperature of the gas. The constraints that the presence of dust put on the molecular emission model are discussed. The following processes are found to have an effect of more than 10% on the integrated intensities (relative to a standard model): cooling by ^{13}CO and HCN in carbon stars, cooling by H_2O in oxygen-rich stars, and the location of the inner boundary of the molecular shell. The model including all physical features considered predicts CO(6–5) intensities which are 25% larger and CO(1–0) intensities which are 10% smaller than those of the standard model. Photoelectric heating can be the dominant source of heating in the outer layers, thereby determining the CO(1–0) intensity, depending on the beam size of the telescope and the efficiency of the shielding of UV radiation by dust.

Key words: circumstellar matter – stars: late type – radio lines: stars – stars: AGB, post-AGB

1. Introduction

Knowledge of the mass loss rate of AGB stars is crucial in understanding their evolution, because mass loss effectively determines the lifetime of a star on the AGB. The mass loss rate can be deduced from modelling the dust emission (e.g. Bedijn 1987; Schutte & Tielens 1989; Justtanont & Tielens 1992; Griffin 1993) or the molecular line emission. With regard to the latter, detailed models for individual stars have been proposed (IRC 10 216: Kwan & Hill 1977 (KH); Kwan & Linke 1982 (KL); Sahai 1987; Huggins et al. 1988; Truong-bach et al. 1991; U Cam: Sahai 1990; AFGL 2688: Truong-bach et al. 1990) or the convenient formula of Knapp & Morris (1985, KM) to calculate the mass loss rate has been widely used. Recently, Kastner (1992) presented an improved simple fit formula to determine the mass loss rate.

Send offprint requests to: M.A.T. Groenewegen at IAP address

The KM-formula is based on the assumption that the kinetic temperature derived for the infrared carbon star IRC 10 216 holds for other stars (including oxygen-rich ones) as well. It has been shown however that the kinetic temperature structure can be very different from that in IRC 10 216 (Sahai 1990; Jura et al. 1988 (JKO); Kastner 1992). Evidently, the kinetic temperature is strongly coupled to the molecular excitation calculation.

In this paper the heating and cooling mechanisms and the assumptions involved in calculating the kinetic temperature and the influence of them on the line profiles are investigated. The constraints that the presence of dust puts on molecular models are discussed. The main differences with the recent similar work of Kastner (1992) are in the exact treatment of the cooling by CO and the inclusion of the photoelectric effect.

In Sect. 2 all necessary theoretical ingredients are presented. In Sect. 3 the different components involved in the heating and cooling calculations and their influence on the line profiles are investigated. The results are discussed in Sect. 4.

2. Theory

2.1. The molecular excitation program

The model described by Morris et al. (1985) is used to calculate the level populations. The main assumptions are spherical symmetry and that the Sobolev approximation is valid (this presumes that the local linewidth is much smaller than the expansion velocity). The molecules are excited by: (1) collisions with H_2 molecules, (2) interaction with the 2.8 K background radiation, and (3) infrared radiation from a central blackbody of temperature T_{BB} and radius R_{BB} which leads to pumping from the $v = 0$ vibrational state into the $v = 1$ state.

The original model of Morris et al. was changed to incorporate the following effects:

1. In the original model the velocity law was used to calculate the radiation intensities in the vibrational and rotational lines but was not used in the density calculation. This was changed to give $n(r) \sim r^{-2} v^{-1}$ instead of the original $n(r) \sim r^{-2}$.
2. Helium is taken into account as a collision partner. The CO + He and HCN + He collisional cross sections are taken from Green & Chapman (1978) and Green & Thaddeus (1974),

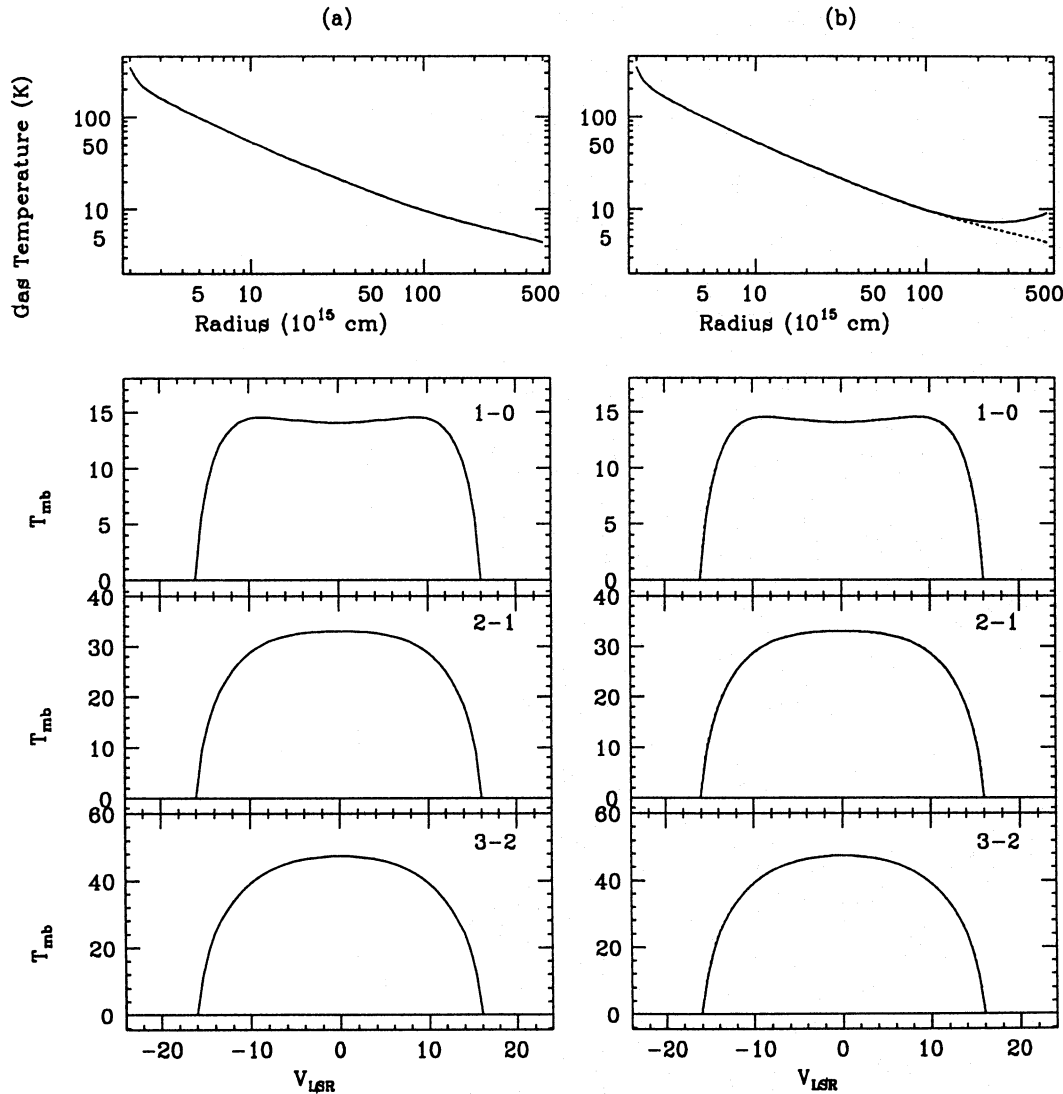


Fig. 1a and b. The temperature structure and CO line profiles for, **a** the standard Kwan & Hill (KH) case, and **b** when photoelectric heating is included. There is no change in the line profiles, only in the temperature structure. In panel **b** the standard KH case is represented by the dotted line. All profiles are calculated for a 30m telescope

rapidly (see Habing et al. 1994). The molecular emission originates from several tens to hundreds of stellar radii where F_λ is almost independent of the radial distance.

Radiative pumping of molecules is provided by thermal emission from hot dust close to the star. In molecular emission models this is represented by a blackbody of temperature T_{BB} and radius R_{BB} . These quantities can be estimated from the DRT-models. At each gridpoint in the DRT-model the blackbody temperature of the radiation field is determined. In this way a realistic estimate of T_{BB} and R_{BB} is obtained. Finally, DRT-models provide $\tau_{0.1}$, which is needed to calculate the photoelectric heating (Eq. 10) and the dust temperature profile which is needed in the heating rate due to the gas-dust temperature difference (Eq. 7).

3. The relation between gas kinetic temperature and line profiles

In this section the influence of the different components involved in calculating the gas kinetic temperature are investigated. The model of KH for IRC 10 216 will be the reference case. The aim of this section is not to re-investigate IRC 10 216 but the KH results are the best documented regarding heating- and cooling rates and the temperature structure.

The parameters in the KH model are: luminosity $L = 21\,000 L_\odot$, distance $D = 200$ pc, mass loss rate $\dot{M} = 2\,10^{-5} M_\odot \text{ yr}^{-1}$, dust-to-gas ratio $\Psi = 0.01$, grain radius $a = 0.1 \mu\text{m}$, grain density $\rho_d = 1 \text{ g cm}^{-3}$, absorption efficiency $Q = 0.013$. The inner boundary condition is $T = 350 \text{ K}$ at $2\,10^{15} \text{ cm}$. The adiabatic index is $\gamma = 5/3$. The CO abundance is $f_{CO} = 8\,10^{-4}$ and is constant between $r_{inner} = 2\,10^{15}$ and $r_{outer} = 5\,10^{17} \text{ cm}$. The velocity law is $v(r) = 16.0(1 -$

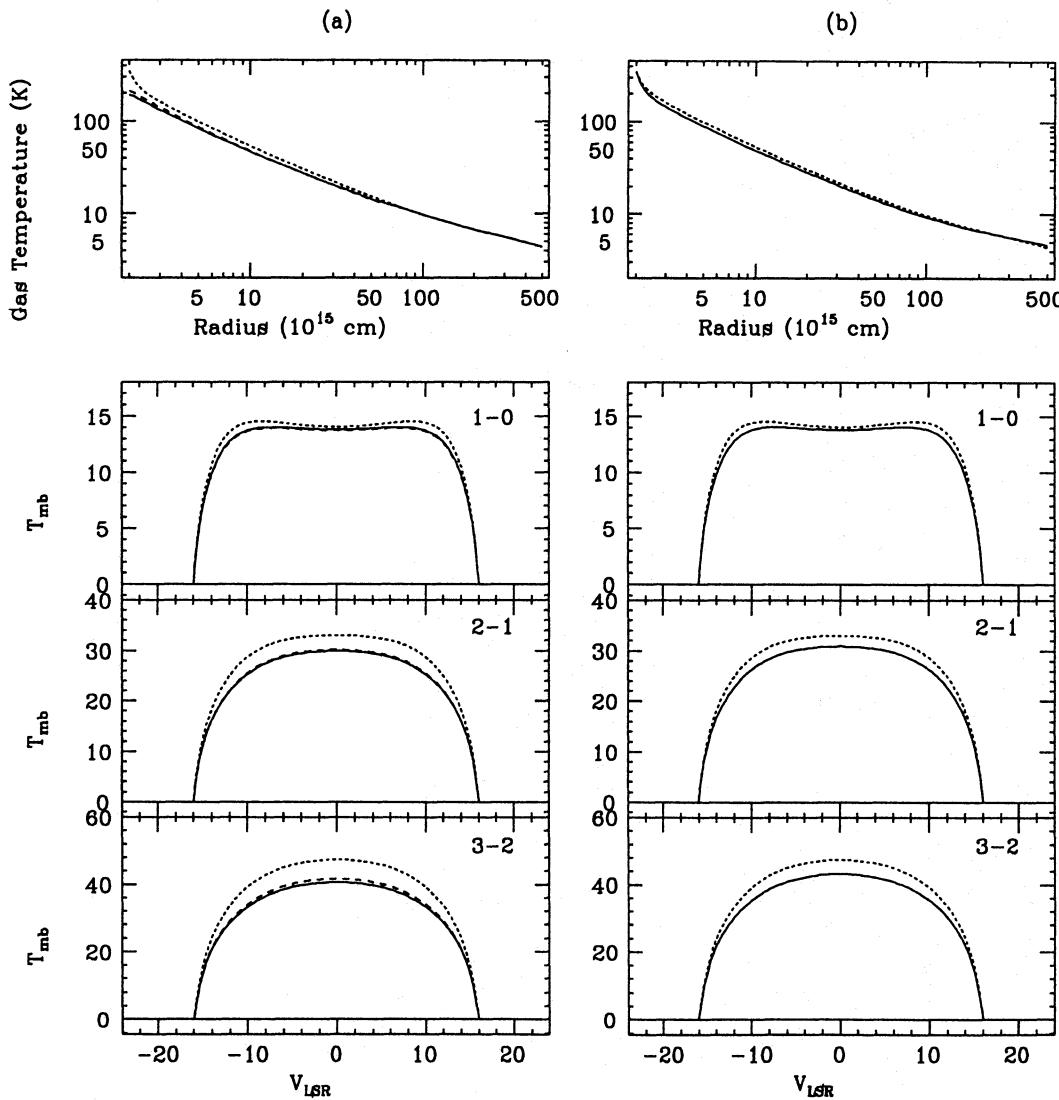


Fig. 2a and b. The temperature structure and CO line profiles when, **a** water cooling is included with an abundance $f_{\text{H}_2\text{O}} = 5 \cdot 10^{-4}$ (solid line) and $f_{\text{H}_2\text{O}} = 1.2 \cdot 10^{-3}$ (dashed line), and **b** cooling by ^{13}CO and HCN is included (without H_2O cooling). The dotted line indicates the standard KH case

$\frac{4 \cdot 10^{14} \text{ cm}}{r} \cdot 0.5 \text{ km s}^{-1}$, but in the heating and cooling calculations KH assumed $v = \text{constant} = 16.0 \text{ km s}^{-1}$ and neglected the drift velocity (see Eq. 5). The central blackbody for calculating the infrared excitation is a 650 K blackbody of radius $6 \cdot 10^{14} \text{ cm}$ for CO and a 300 K, $3 \cdot 10^{15} \text{ cm}$ blackbody for HCN (again, all parameters taken from the KH model). Cooling by H_2 , ^{13}CO and HCN is neglected and there is no helium or H_2O present. Heating by the photoelectric effect, cosmic rays and the temperature difference between the gas and the dust are neglected. For the effective temperature a value of $T_{\text{eff}} = 2300 \text{ K}$ is assumed (Ridgway & Keady 1988). The CO + H₂ and HCN + H₂ collision rates are taken from Green & Thaddeus (1974, 1976). KH did not explicitly state how they extrapolated the CO cross sections; I used the fit by de Jong et al. (1975).

The results of this standard case regarding the temperature structure and the CO(1-0), CO(2-1) and CO(3-2) pro-

files are shown in Fig. 1a. The profiles have been calculated for a 30m telescope (HPBW = 23'' at 115 GHz, corresponding to a linear radius of $3.4 \cdot 10^{16} \text{ cm}$ at 200 pc). For the standard case I find a heating rate (neglecting the drift velocity in Eq. 5) per H₂ molecule of $7.5 \cdot 10^{-26} \text{ erg s}^{-1}$ and a cooling rate of $5.1 \cdot 10^{-26} \text{ erg s}^{-1}$ at $1 \cdot 10^{17} \text{ cm}$. KH find $7.4 \cdot 10^{-26}$ and $4.6 \cdot 10^{-26} \text{ erg s}^{-1}$, respectively. The gas temperature and CO(1-0) excitation temperature in the model are 9.73 and 8.39 K at $1 \cdot 10^{17} \text{ cm}$, 4.92 and 2.86 K at $4 \cdot 10^{17} \text{ cm}$. KH find 9.8 K, 8.1 K and 5.0 K, 2.8 K, respectively. The model results agree excellently with KH, the small differences are probably due to numerical details in the two codes.

In the following subsections the influence of several assumptions on the temperature structure and the CO line profiles is investigated. In Table 2 the changes in the integrated intensity ($\int T d\nu$) relative to the standard case are tabulated for the low-

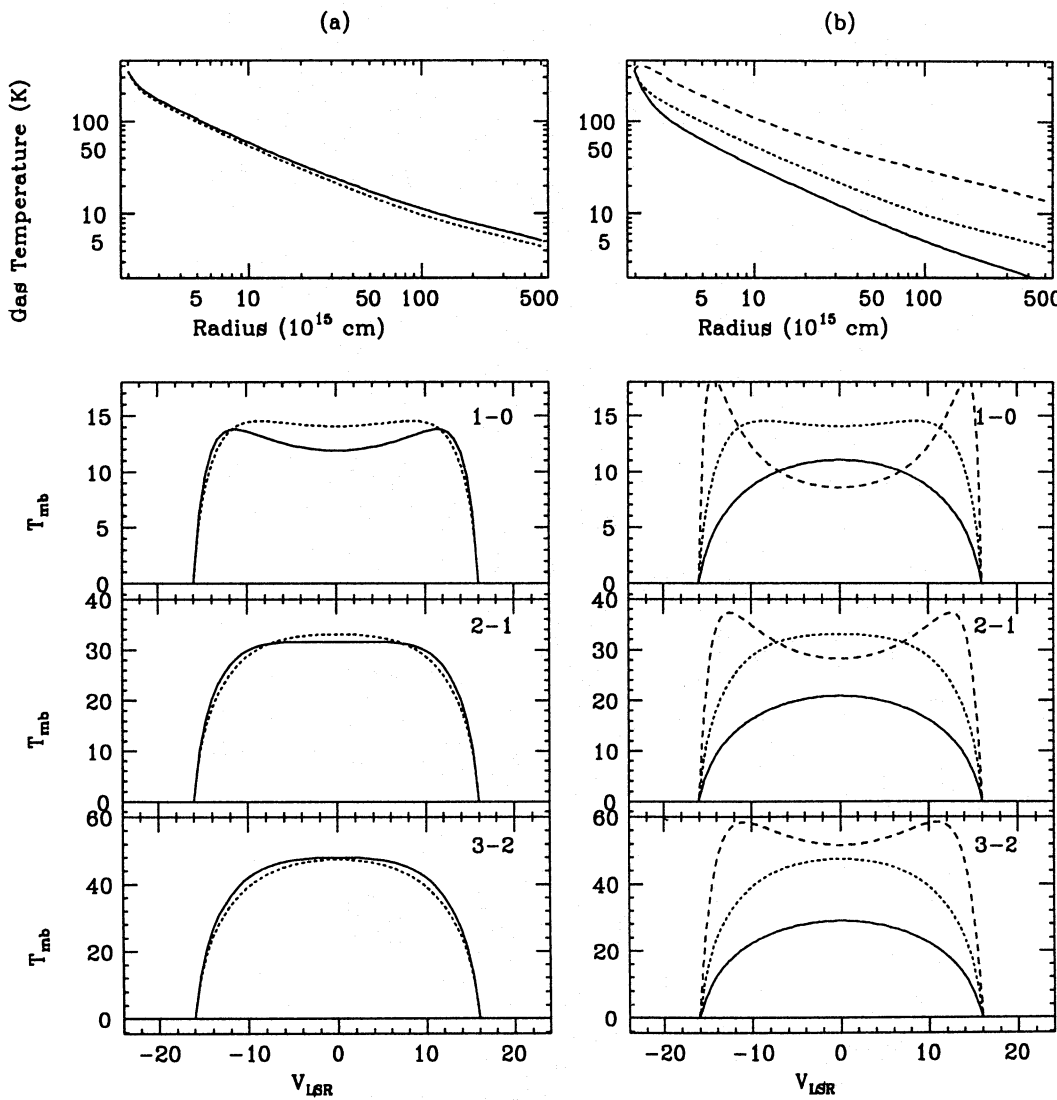


Fig. 3a and b. The temperature structure and CO line profiles when, **a** an helium abundance $f_{\text{He}} = 0.1$ is included, and **b** the mass loss rate and absorption efficiency are changed: $\dot{M} = 4 \cdot 10^{-5} M_{\odot} \text{ yr}^{-1}$, $Q = 0.0065$ (solid line) or $\dot{M} = 1 \cdot 10^{-5} M_{\odot} \text{ yr}^{-1}$, $Q = 0.026$ (dashed line). The dotted line is the standard KH case

est six transitions of ^{12}CO . In Figs. 1-4 the temperature structure and line profiles are shown for selected models.

3.1. The velocity law and drift velocity

KH assumed $v(r) = \text{constant}$ and neglected a term of the order $1/(1 + v_{\text{dr}}/v)$ in the heating calculation. This results in an overestimate of the heating rate (Eq. 5). When the velocity law and the drift velocity are properly taken into account, lower temperatures and less emission are expected. The intensities are reduced by 5–10%.

3.2. Heating by the photoelectric effect

When UV radiation can penetrate the outer layers of the envelope the photoelectric effect on grains can become important. The heating rate is given by Eqs. 10–12. Since KH assumed

a constant CO abundance, the electron density would be very small (as the net production of electrons by grains is negligible, cf. de Jong 1977) and there would be almost no photoelectric effect ($\gamma \rightarrow \infty$, $x \rightarrow 1$, $H_{\text{pe}} \rightarrow 0$). In order to get an estimate of the heating rate a value of $x = 0.7$ was assumed (Eq. 10). This gives a heating rate similar to the one adopted by KL and Truong-Bach et al. (1990). The parameter $\tau_{0.1}$ was estimated from Ridgway & Keady (1988) who derived a dust optical depth of 5.5 at 2 μm and an inner dust radius of $5R_{\ast}$ for IRC 10 216. Extrapolating the optical depth to 0.1 μm using the absorption efficiency of amorphous carbon (Rouleau & Martin 1991) which is appropriate for IRC 10 216 (Martin & Rogers 1987; Orofino et al. 1990; Griffin 1990), leads to an optical depth of 730 at the inner dust radius, or $\tau_{0.1} = 2.3 \cdot 10^{17} \text{ cm}/r$. This calculation neglects scattering. When scattering is important, which depends on the grain size, the optical depth at 0.1 μm will be larger. The line

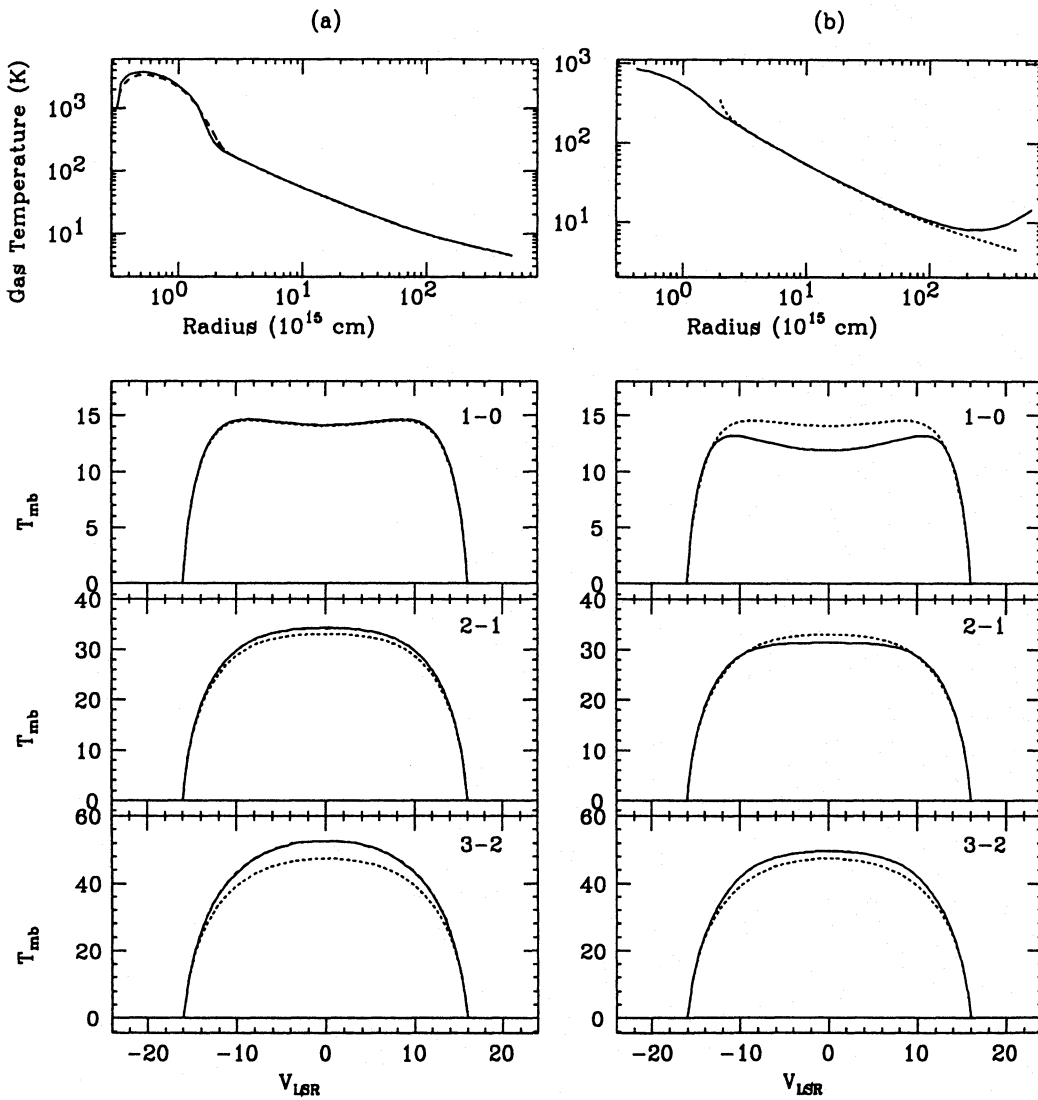


Fig. 4a and b. The temperature structure and CO line profiles when, **a** the inner boundary is $T = 1000$ K at $3.2 \cdot 10^{14}$ cm with $\gamma = 5/3$ for all temperatures (solid line) and **b** the ‘combined’ model including all physics (see Sect. 3.12 for all details). The dotted line is the standard KH case

profiles and temperature structure are shown in Fig. 1b, which clearly illustrates the heating in the outer layers. *In this particular case*, photoelectric heating has a negligible effect on the line intensities because the beam size ($3.4 \cdot 10^{16}$ cm) is smaller than the region where the temperature is increased ($> 2.3 \cdot 10^{17}$ cm). The $^{12}\text{CO}(1-0)$ integrated intensity is raised by 0.1%.

The photoelectric effect is a potentially important heating mechanism in the outer layers, but the effect on the (1-0) profile depends on the telescope beam size relative to the region where the UV radiation can effectively penetrate, which in turn depends on the uncertain contribution of scattering to the dust opacity at UV wavelengths. This means that the influence of the photoelectric effect on the line profiles is not easy to predict as it depends both on the distance to the object and the beam size of the telescope.

3.3. Heating by cosmic rays

This effect is totally negligible in this case. The temperature at the outer radius is raised by only 0.3 K compared to the standard case. The (1-0) integrated intensity is raised by 0.1%.

3.4. Heating by the gas-dust temperature difference

To estimate the effect of this process (Eq. 7), a dust temperature profile has to be adopted. From Griffin (1990) it is derived that for IRC 10 216 $T_d = 530(r/10^{15} \text{ cm})^{-0.413}$ is a good approximation.

The effect is non-negligible. The intensities are raised by up to 10 percent. The ratio of the heating rates $H_{\Delta T}/H_{dg}$ is 0.10 at the inner radius and 0.04 at 10^{17} cm.

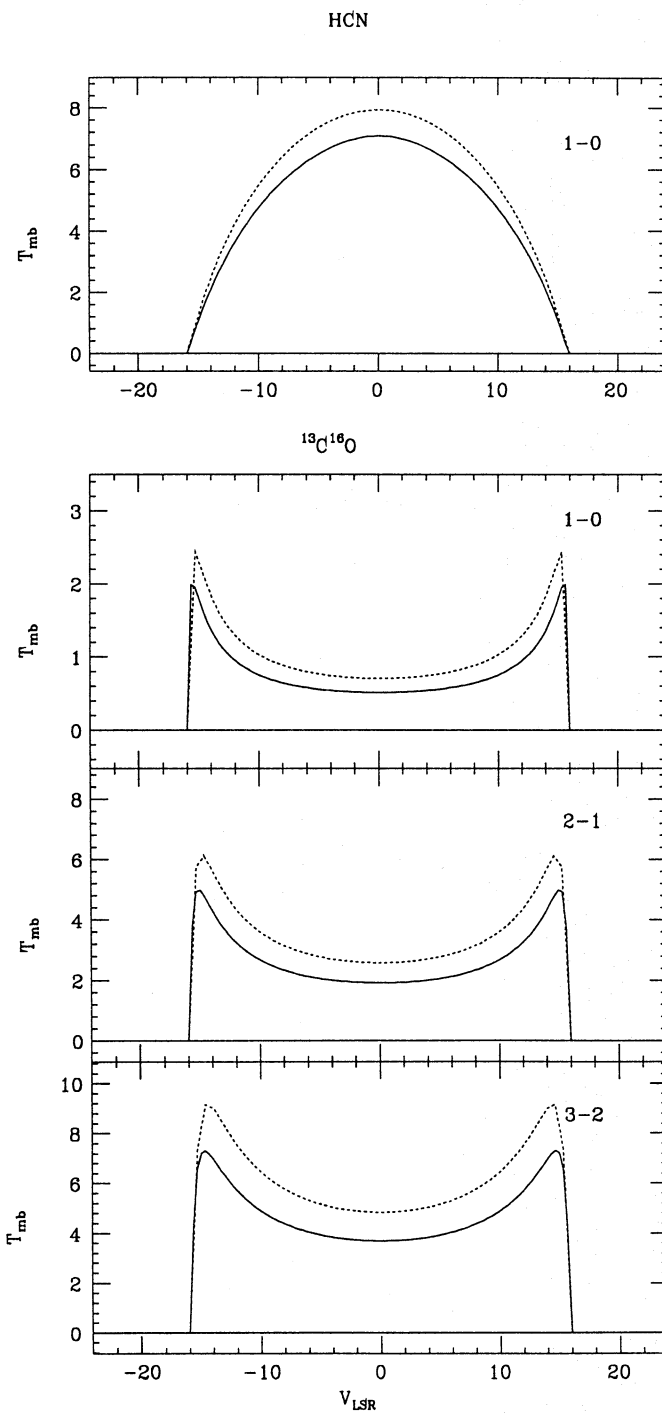


Fig. 5. The HCN and ^{13}CO line profiles for the combined model (solid line) and the standard KH case (dotted line)

ously fitting the spectral energy distribution and the molecular line emission profiles is potentially the most accurate method to determine the mass loss rate in AGB stars.

Acknowledgements. I thank Mark Morris for providing a copy of his numerical code and subsequent support and Xander Tielens for his comments on the treatment of water cooling and the photoelectric effect and for his interest in this project. Teije de Jong and René Oudmaijer are thanked for comments on the manuscript. The research of MG was

supported under grant 782-373-030 by the Netherlands Foundation for Research in Astronomy (ASTRON), which is financially supported by the Netherlands Organisation for Scientific Research (NWO).

Appendix A: H_2O rotational cooling

I re-derive the equations to calculate the excitation temperature of a H_2O molecule and present the equation to calculate the cooling rate. This treatment is a generalization of the description by Goldreich & Scoville (1976, GS) and Tielens (1983). The calculation is based on the classical treatment of the H_2O molecule and assumes that all rotational levels in the ground vibrational state have the same excitation temperature T_x . With T_x determined, the cooling rate per unit volume is given by (GS Eq. 11, Tielens Eq. 15):

$$C_{\text{H}_2\text{O}} = n_{\text{H}_2}(1 + \sqrt{2}f_{\text{He}})n_{\text{H}_2\text{O}} \times \langle\sigma v\rangle h\nu \left(e^{-h\nu/kT} - e^{-h\nu/kT_x} \right) \quad (\text{A1})$$

where n_{H_2} and $n_{\text{H}_2\text{O}}$ are the number densities of the respective molecules, f_{He} is the helium abundance relative to hydrogen and $\langle\sigma v\rangle$ is the $\text{H}_2\text{-H}_2\text{O}$ inelastic collisional rate constant which is set to $\langle\sigma v\rangle = 2.0 \cdot 10^{-11} T^{1/2} \text{ cm}^3 \text{ s}^{-1}$ (GS). The $\text{He-H}_2\text{O}$ collisional rate is assumed to be a factor $\sqrt{2}$ lower due to the difference in mass. The frequency ν is the classical value of the rotational frequency of an H_2O molecule whose rotational energy is $3kT_x/2$, or:

$$\nu = \nu_0 T_x^{1/2} \quad (\text{A2})$$

In the derivation of the excitation temperature I closely follow GS. The idealised water molecule has three scalar levels, two rotational levels in the ground vibrational state and one rotational level in the excited vibrational state. The rate equations are given by (GS Eq. A1):

$$\begin{aligned} \frac{dn_1}{dt} &= \beta_{21} A_{21} n_2 + (A_{31} + B_{31} J_{13}) n_3 \\ &\quad - B_{13} J_{13} n_1 - C[n_1 \exp(-h\nu_{21}/kT) - n_2] \\ \frac{dn_2}{dt} &= -\beta_{21} A_{21} n_2 + (A_{32} + B_{32} J_{23}) n_3 \\ &\quad - B_{23} J_{23} n_2 + C[n_1 \exp(-h\nu_{21}/kT) - n_2] \\ \frac{dn_3}{dt} &= B_{13} J_{13} n_1 + B_{23} J_{23} n_2 \\ &\quad - (A_{31} + B_{31} J_{13} + A_{32} + B_{32} J_{23}) n_3 \\ n_1 + n_2 + n_3 &= n \end{aligned} \quad (\text{A3})$$

where $C = \langle\sigma v\rangle n_{\text{H}_2}(1 + \sqrt{2}f_{\text{He}})$. The molecular levels are numbered 1, 2 and 3 in order of increasing energy. The net radiative decay rate is given by $\beta_{21} A_{21}$, where A_{21} is the spontaneous decay rate of level 2, and β_{21} is the probability that a photon escapes without further interaction. GS verified that the rotational transitions are optically thick and using the Sobolev approximation (Castor 1970), the term $\beta_{21} A_{21}$ is given by (GS Eq. A5):

$$\beta_{21} A_{21} = \frac{16\pi\nu(r)}{3r\lambda_{21}^3(n_1 - n_2)} (1 + 0.5\epsilon) \quad (\text{A4})$$

- de Jong T., Chu S.I., Dalgarno A., 1975, ApJ 199, 69
de Jong T., 1977, A&A 55, 137
Jura M., Kahane C., Omont A., 1988, A&A 201, 80 (JKO)
Justtanont K., Tielens A.G.G.M., 1992, ApJ 389, 400
Kastner J.H., 1992, ApJ 401, 337
Knapp G.R., Morris M., 1985, ApJ 292, 640
Kwan J., Hill F., 1977, ApJ 215, 781 (KH)
Kwan J., Linke R.A., 1982, ApJ 254, 587 (KL)
Mamon M., Glassgold A.E., Huggins P.J., 1988, ApJ 328, 797
Martin P.G., Rogers C., 1987, ApJ 322, 374
Morris M., Lucas R., Omont A., 1985, A&A 142, 107
Nejad L.A.M., Miller T.J., 1988, MNRAS 230, 79
Nercessian E., Guilloteau S., Omont A., Benayoun J.J., 1989, A&A 210, 225
Netzer N., Knapp G.R., 1987, ApJ 323, 734
Nyman L.-A., 1993, A&A 269, 377
Orofino V., Colangeli L., Bussoletti E., Blanco A., Fonti S., 1990, A&A 231, 105
Ridgway S.T., Keady J.J., 1988, ApJ 326, 843
Rouleau F., Martin P.G., 1991, ApJ 377, 526
Sahai R., 1987, ApJ 318, 809
Sahai R., 1990, ApJ 362, 652
Schutte W.A., Tielens A.G.G.M., 1989, ApJ 343, 369
Tielens A.G.G.M., 1983, ApJ 271, 702
Tielens A.G.G.M., Hollenbach D., 1985, ApJ 291, 722
Truong-Bach, Morris D., Nguyen-Q-Rieu, Deguchi S., 1990, A&A 230, 431
Truong-Bach, Morris D., Nguyen-Q-Rieu, 1991, A&A 249, 435